

# TWO-STEP LATTICE SUPER-EXPONENTIAL ALGORITHM FOR BLIND EQUALIZATION OF MULTI-INPUT MULTI-OUTPUT CHANNELS

Chong-Yung Chi, Faa-Yeu Wang and Meng-Chian Chiang

Department of Electrical Engineering  
National Tsing Hua University, Hsinchu, Taiwan, R.O.C.  
Tel: 886-3-5731156, Fax: 886-3-5751787, E-mail: cychi@ee.nthu.edu.tw

**Abstract** - Feng and Chi reported a two-step lattice super-exponential algorithm (2S-LSEA) for blind equalization of single-input single-output (SISO) channels that is superior to Shalvi and Weinstein's FIR filter based super-exponential algorithm (SEA) in faster convergence speed, lower computational complexity, and more reliable performance to a variety of channels, besides modularity and low sensitivity to parameter quantization effects of lattice structure. In this paper, a 2S-LSEA for multi-input multi-output (MIMO) channels is proposed that is also superior to Yeung and Yau's SEA for MIMO channels in the same preceding advantages of the 2S-LSEA for SISO channels. Some simulation results are presented to support the efficacy of the proposed 2S-LSEA for MIMO channels.

## I. Introduction

Multichannel blind equalization (deconvolution) is a crucial signal processing procedure to mitigate the multipath fading, multiple access interference (MAI) and noise effects of multiuser communication systems with only measurements  $\mathbf{x}[n]$  ( $P \times 1$  vector) given by

$$\begin{aligned} \mathbf{x}[n] &= \mathbf{H}[n] * \mathbf{u}[n] + \mathbf{w}[n] \\ &= \sum_{k=-\infty}^{\infty} \mathbf{H}[k] \mathbf{u}[n-k] + \mathbf{w}[n] \end{aligned} \quad (1)$$

where  $\mathbf{H}[n]$  ( $P \times K$  matrix) is the impulse response of an unknown multi-input multi-output (MIMO) linear time-invariant (LTI) channel,  $\mathbf{u}[n]$  ( $K \times 1$  vector) includes the  $K (\leq P)$  users' transmitted signals (symbol streams)  $u_1[n], u_2[n], \dots, u_K[n]$ , and  $\mathbf{w}[n]$  ( $P \times 1$  vector) is additive noise. The MIMO linear FIR equalizer, denoted by  $\mathbf{V}[n]$  ( $K \times P$  matrix), of order  $L$  has been widely used to process  $\mathbf{x}[n]$  such that the equalizer out-

put

$$\mathbf{e}[n] = \mathbf{V}[n] * \mathbf{x}[n] = \sum_{i=0}^L \mathbf{V}[i] \mathbf{x}[n-i] \quad (2)$$

approximates a permutation of  $(\alpha_1 u_1[n - \tau_1], \alpha_2 u_2[n - \tau_2], \dots, \alpha_K u_K[n - \tau_K])^T$  where  $\alpha_j$ 's are unknown scale factors and  $\tau_j$ 's are unknown time delays.

Shalvi and Weinstein [1,2] proposed a computationally efficient iterative super-exponential algorithm (SEA) for single-input single-output (SISO) ( $K = P = 1$ ) channels. It has been extended to the corresponding fractionally-spaced algorithm by Gomes and Barroso [3] as well as MIMO blind deconvolution algorithm by Yeung and Yau [4] with applications to wireless communications. Yeung and Yau's SEA for MIMO systems is also a multistage successive cancellation algorithm, but its software and hardware implementation is still limited by computational complexity.

Recently, Feng and Chi [5] proposed a two-step lattice SEA (2S-LSEA) for SISO systems that is superior to the SEA due to much faster convergence speed, much lower computational complexity, and more reliable performance to a variety of channels in addition to modularity and low sensitivity to parameter quantization effects of lattice structure [6]. In this paper, we further propose a 2S-LSEA for MIMO channels that also shares the advantages of the 2S-LSEA for SISO channels.

## II. Review of SEA for MIMO Channels

Assume that we are given a set of measurements  $\mathbf{x}[n]$ ,  $n = 0, 1, \dots, N-1$  in the absence of noise and that  $\mathbf{V}[n]$  is an  $L$ th-order  $K \times P$  linear FIR filter with the  $(k, j)$ th component denoted by  $v_{k,j}[n]$ . Let

$$\mathbf{x}_j[n] = (x_j[n], x_j[n-1], \dots, x_j[n-L])^T \quad (3)$$

$$\mathbf{v}_{k,j} = (v_{k,j}[0], v_{k,j}[1], \dots, v_{k,j}[L])^T \quad (4)$$

This work was supported by the National Science Council under Grant NSC-89-2213-E-007-093.

where  $x_j[n]$  is the  $j$ th entry of  $\mathbf{x}[n]$ . Then the  $k$ th entry of  $\mathbf{e}[n]$  can be expressed as

$$e_k[n] = \sum_{j=1}^P v_{k,j}[n] * x_j[n] = \sum_{j=1}^P \mathbf{v}_{k,j}^T \mathbf{x}_j[n] \quad (5)$$

$$= \sum_{j=1}^K s_{k,j}[n] * u_j[n] \quad (6)$$

where

$$s_{k,j}[n] = \sum_{m=1}^P \sum_{l=0}^L v_{k,m}[l] h_{m,j}[n-l] \quad (7)$$

where  $h_{m,j}[n]$  is the  $(m, j)$ th component of  $\mathbf{H}[n]$ . Next, let us present the multistage successive cancellation (MSC) procedure [7] in which the SEA for MIMO channels is employed for obtaining the optimum  $\mathbf{e}[n]$ .

### MSC Procedure

At the  $\kappa$ th stage, the MSC procedure includes the following two steps:

(T1) Find one input estimate, said  $\hat{u}_q[n]$  (where  $q$  is unknown), and the associated channel estimates  $\hat{h}_{j,q}[n]$ ,  $j = 1, 2, \dots, P$  using the iterative SEA for MIMO channels.

(T2) Cancellation of  $\hat{u}_q[n]$ . Update  $x_j[n]$  by  $x_j[n] - \hat{u}_q[n] * \hat{h}_{j,q}[n]$ ,  $j = 1, 2, \dots, P$  such that the resulting  $\mathbf{x}[n]$  corresponds to the output of a  $P \times (K - \kappa)$  channel.

All the estimates  $\hat{u}_1[n]$ ,  $\hat{u}_2[n]$ , ...,  $\hat{u}_K[n]$  are obtained in a non-sequential order through  $K$  stages. Next, let us briefly review the iterative SEA for MIMO channels used in (T1).

### SEA for MIMO Channels

Assume that  $\mathbf{x}[n]$  is the output of a  $P \times (K - \kappa + 1)$  channel and  $\hat{u}_q[n]$  will be estimated at stage  $\kappa$ . Let

$$\boldsymbol{\nu} = (\mathbf{v}_{q,1}^T, \mathbf{v}_{q,2}^T, \dots, \mathbf{v}_{q,P}^T)^T \quad (8)$$

Assume that the  $(i-1)$ th iteration of the SEA for MIMO channels ended up with the equalized signal  $e_q^{[i-1]}[n]$  (see (5)) associated with  $\boldsymbol{\nu}_{i-1}$ . At the  $i$ th iteration,  $\boldsymbol{\nu}_i$  is updated by

$$\boldsymbol{\nu}_i = \frac{\tilde{\mathbf{R}}^{-1} D_q}{\|\tilde{\mathbf{R}}^{-1} D_q\|} \quad (9)$$

where  $\tilde{\mathbf{R}}$  is a  $P(L+1) \times P(L+1)$  matrix given by

$$\tilde{\mathbf{R}} = \begin{bmatrix} R_{1,1} & R_{1,2} & \dots & R_{1,P} \\ R_{2,1} & R_{2,2} & \dots & R_{2,P} \\ \vdots & \vdots & \ddots & \vdots \\ R_{P,1} & R_{P,2} & \dots & R_{P,P} \end{bmatrix} \quad (10)$$

where

$$R_{i,j} = E\{\mathbf{x}_i[n] \mathbf{x}_j^H[n]\} \quad (11)$$

$$D_q = (\mathbf{d}_{q,1}^T, \mathbf{d}_{q,2}^T, \dots, \mathbf{d}_{q,P}^T)^T \quad (12)$$

in which

$$\mathbf{d}_{q,p} = C_4\{e_q^{[i-1]}[n], \mathbf{x}_p[n]\} \quad (13)$$

where  $C_4\{w, \mathbf{z}\}$  denotes the fourth-order joint cumulant of random variable  $w$  and random vector  $\mathbf{z}$  as follows

$$C_4\{w, \mathbf{z}\} = \text{cum}\{w, w, w^*, \mathbf{z}^*\}. \quad (14)$$

As the algorithm converges, the optimum estimate

$$\hat{u}_q[n] = e_q^{[i]}[n] = \alpha u_q[n - \tau] \quad (15)$$

is obtained, and the associated amount of interference ISI( $e_q^{[i]}[n]$ ) (in the absence of noise) also converges to zero at a super-exponential rate, where

$$\text{ISI}(e_q[n]) = \frac{\{\sum_{j,n} |s_{q,j}[n]|^2\} - \max_{j,n} \{|s_{q,j}[n]|^2\}}{\max_{j,n} \{|s_{q,j}[n]|^2\}} \quad (16)$$

Then  $h_{j,q}[k]$  can be estimated as

$$\hat{h}_{j,q}[k] = \frac{E[x_j[n+k] \hat{u}_q^*[n]]}{E[|\hat{u}_q[n]|^2]}, \quad j = 1, 2, \dots, P. \quad (17)$$

## III. 2S-LSEA for MIMO Channels

### A. MIMO Lattice Filter

The LSEA and 2S-LSEA for MIMO channels to be presented below begin with Friedlander's MIMO lattice LPE filter [8] that is summarized as follows:

$$\mathbf{f}_{m+1}[n] = \mathbf{f}_m[n] - K_{m+1}^b \mathbf{b}_m[n-1] \quad (18)$$

$$\mathbf{b}_{m+1}[n] = \mathbf{b}_m[n-1] - K_{m+1}^{fH} \mathbf{f}_m[n] \quad (19)$$

$$K_{m+1}^b = \Delta_{m+1} (R_m^b)^{-1} \quad (20)$$

$$K_{m+1}^f = (R_m^f)^{-1} \Delta_{m+1} \quad (21)$$

$$\Delta_{m+1} = E\{\mathbf{f}_m[n] \mathbf{b}_m^H[n-1]\} \quad (22)$$

$$R_m^f = E\{\mathbf{f}_m[n] \mathbf{f}_m^H[n]\} \quad (23)$$

$$R_m^b = E\{\mathbf{b}_m[n-1] \mathbf{b}_m^H[n-1]\} \quad (24)$$

Two remarks regarding this MIMO lattice LPE filter are worth mentioning as follows:

- (R1) As the SISO lattice LPE filter [6], it also shares the modularity and low sensitivity to parameter quantization effects.
- (R2) The forward prediction error  $\mathbf{f}_m[n]$  ( $P \times 1$  vector) approximates a white vector random process for sufficiently large  $m$ . The backward prediction error  $\mathbf{b}_m[n]$  ( $P \times 1$  vector) is uncorrelated with  $\mathbf{b}_l[n]$  for  $m \neq l$ .

Some modifications to  $\mathbf{f}_m[n]$  and  $\mathbf{b}_m[n]$  are needed for the LSEA to be presented below. Let

$$\hat{\mathbf{f}}_m[n] = U_f \mathbf{f}_m[n] \quad (25)$$

$$\hat{\mathbf{b}}_m[n-1] = U_b \mathbf{b}_m[n-1] \quad (26)$$

where  $U_f$  and  $U_b$  are  $P \times P$  matrices such that

$$D_m^f = E\{\hat{\mathbf{f}}_m[n] \hat{\mathbf{f}}_m^H[n]\} = U_f R_m^f U_f^H \quad (27)$$

$$D_m^b = E\{\hat{\mathbf{b}}_m[n-1] \hat{\mathbf{b}}_m^H[n-1]\} = U_b R_m^b U_b^H \quad (28)$$

are diagonal. The linear transformation matrices  $U_f$  and  $U_b$  can be found through the Gram-Schmidt orthogonalization procedure. Moreover,  $\mathbf{f}_{m+1}[n]$  given by (18) and  $\mathbf{b}_{m+1}[n]$  given by (19) can be simplified as

$$\mathbf{f}_{m+1}[n] = \mathbf{f}_m[n] - E\{\mathbf{f}_m[n] \hat{\mathbf{b}}_m^H[n-1]\} \cdot [D_m^b]^{-1} \hat{\mathbf{b}}_m[n-1] \quad (29)$$

$$\mathbf{b}_{m+1}[n] = \mathbf{b}_m[n-1] - E\{\mathbf{b}_m[n-1] \hat{\mathbf{f}}_m^H[n]\} \cdot [D_m^f]^{-1} \hat{\mathbf{f}}_m[n] \quad (30)$$

that are actually free from matrix inversion since  $D_m^b$  and  $D_m^f$  are diagonal. As a final remark, (R2) also applies to  $\hat{\mathbf{f}}_m[n]$  and  $\hat{\mathbf{b}}_m[n]$ . The modified MIMO LPE filter is also shown in Figure 1.

### B. LSEA for MIMO Channels

Two versions of the LSEA for MIMO channels are to be presented. The one, denoted by LSEA-B, processes  $\hat{\mathbf{b}}_j[n]$  to obtain the equalized signal  $e_q[n]$ , and the other, denoted by LSEA-F, processes  $\hat{\mathbf{f}}_j[n]$  to obtain  $e_q[n]$ .

#### LSEA-B:

As shown in Figure 2, the equalized signal  $e_q[n]$  is obtained by

$$e_q[n] = \sum_{j=0}^L \mathbf{c}^T[j] \hat{\mathbf{b}}_j[n] \quad (31)$$

Let

$$\boldsymbol{\nu} = (\mathbf{c}^T[0], \mathbf{c}^T[1], \dots, \mathbf{c}^T[L])^T \quad (32)$$

The LSEA-B for MIMO channels is nothing but the SEA for MIMO channels presented in Section II with  $\mathbf{x}_j[n]$  ( $(L+1) \times 1$  vector) replaced by  $\hat{\mathbf{b}}_j[n]$  ( $P \times 1$  vector) and  $\mathbf{v}_{i,j}$  ( $(L+1) \times 1$  vector) replaced by  $\mathbf{c}[j]$  ( $P \times 1$  vector). At the  $i$ th iteration,  $\boldsymbol{\nu}_i$  is also updated by (9) in which

$$\tilde{R} = \text{Diag}(D_0^b, D_1^b, \dots, D_L^b) \quad (33)$$

$$D_q = (\mathbf{d}_{q,0}^T, \mathbf{d}_{q,1}^T, \dots, \mathbf{d}_{q,L}^T)^T \quad (34)$$

$$\mathbf{d}_{q,l} = C_4 \{e_q^{[i-1]}[n], \hat{\mathbf{b}}_l[n]\} \quad (35)$$

Two worthy remarks are as follows:

- (R3) Remark (R1) also applies to the proposed LSEA-B that is computationally efficient simply because  $\tilde{R}$  is diagonal in the computation of  $\boldsymbol{\nu}_i$ .
- (R4) The performance of the proposed LSEA-B is similar to that of the SEA (in terms of ISI) since the former corresponds to a different implementation of the latter.

#### LSEA-F:

As shown in Figure 3, the equalized signal  $e_q[n]$  is obtained by

$$e_q[n] = \sum_{m=0}^M \mathbf{c}^T[m] \hat{\mathbf{f}}_m[n-m] \quad (36)$$

Let

$$\boldsymbol{\nu} = (\mathbf{c}^T[0], \mathbf{c}^T[1], \dots, \mathbf{c}^T[M])^T \quad (37)$$

Through the same derivations as the LSEA-B, at the  $i$ th iteration,  $\boldsymbol{\nu}_i$  is also updated by (9) in which

$$\tilde{R} = \text{Diag}(D_0^f, D_1^f, \dots, D_J^f) \quad (38)$$

$$D_q = (\mathbf{d}_{q,0}^T, \mathbf{d}_{q,1}^T, \dots, \mathbf{d}_{q,M}^T)^T \quad (39)$$

$$\mathbf{d}_{q,m} = C_4 \{e_q^{[i-1]}[n], \hat{\mathbf{f}}_m[n-m]\} \quad (40)$$

Note that the diagonal  $\tilde{R}$  given by (38) was obtained by the whiteness approximation for  $\hat{\mathbf{f}}_j[n]$  (i.e., an amplitude equalized signal) as mentioned in (R2). In other words, only the channel phase distortion is left to the proposed LSEA-F for further processing, thus leading to the following remark.

- (R5) The proposed LSEA-F to which (R3) also applies can significantly and rapidly reduce the associated ISI (see (16)). However, the resultant ISI may be higher than that associated with the LSEA-B when the whiteness approximation is not very applicable for the chosen  $J$ .

### C. 2S-LSEA for MIMO Channels

The proposed iterative 2S-LSEA for MIMO channels consists of the following two steps:

- (S1) Update  $\nu_i$  (defined as (37)) by (9) using the proposed LSEA-F for iterations  $i = 1, 2, \dots, I$ .
- (S2) Update  $\nu_i$  (defined as (32)) by (9) using the proposed LSEA-B for  $i > I$  with the initial condition  $e_q^{[I]}[n]$  obtained at Step (S1).

Let us conclude this section with the following remark.

- (R6) As mentioned in (R5), the LSEA-F used in (S1) can efficiently reduce the associated ISI (see (16)), and thus is helpful to the convergence speed of the LSEA-B used in Step (S2).

### IV. Simulation Results

Two simulation examples are to be presented to support the efficacy of the proposed LSEA-B and 2S-LSEA for MIMO channels. In each example, a two-input two-output system was considered and non-Gaussian synthetic data  $\mathbf{x}[n]$  were generated with SNR of 20 dB (white Gaussian noise) for each output. Then  $\mathbf{x}[n]$  were processed by the SEA and LSEA-B with  $L = 29$ , and by the 2S-LSEA with  $I = 1$ ,  $J = 24$  and  $M = 24$  for the LSEA-F used in Step (S1) and  $L = 29$  for the LSEA-B used in Step (S2). The initial conditions  $\nu_0$  (see (8), (32) and (37)) used by the three algorithms were equivalent. Then the ISI associated with  $u_1[n]$  was calculated from thirty independent runs.

*Example 1:* The two-input two-output FIR channel  $\mathbf{H}[n]$  (taken from [7]) was given by

$$\begin{aligned} h_{1,1}[n] &= [0.6455, -0.3227, 0.6455, -0.3227] \\ h_{1,2}[n] &= [0.6140, 0.3684] \\ h_{2,1}[n] &= [0, 0.3873, 0.8391, 0.3227] \\ h_{2,2}[n] &= [0, -0.2579, -0.6140, 0.8842, \\ &\quad 0.4421, 0, 0.2579] \end{aligned}$$

The two driving inputs  $u_1[n]$  and  $u_2[n]$  were binary random sequences of  $\{+1, -1\}$  with equal probability (1/2) for +1 and -1, and the data length  $N = 1500$ . The initial condition  $\nu_0$  with  $v_{1,1}[n] = \delta[n - 15]$  and  $v_{1,2}[n] = \delta[n - 15]$  was used by the SEA.

The ISI( $\hat{u}_1[n]$ ) versus iteration number associated with the SEA, LSEA-B and 2S-LSEA are shown in Figures 4(a), 4(b) and 4(c), respectively. One can see, from these figures, that as mentioned in (R4), the results

shown in Figure 4(a) are similar to those shown in Figure 4(b), and that the proposed 2S-LSEA converges faster (spending 2 iterations) than the other two algorithms (spending 3 iterations) although the resultant ISI's are similar for the three algorithms. These results are therefore consistent with (R6).

*Example 2:* In this example,

$$\begin{aligned} h_{1,1}[n] &= [0.4, 1, -0.3, 1.6, -0.4, 0.2, 0.4, -0.4, 0.1] \\ h_{1,2}[n] &= [0.3, 0.2, -0.6, 0.2, -0.3, 0, 0.25, -0.05] \\ h_{2,1}[n] &= [-0.1, 0.8, 1.7, 1, 0.5, 0.9, 0.5, -0.1] \\ h_{2,2}[n] &= [0.3, 0.7, 1.3, 1.5, 1.2, 0.5, 0.4, -0.3, 0.2] \end{aligned}$$

The two driving inputs  $u_1[n]$  and  $u_2[n]$  were 4-QAM random sequences of  $\{\pm 1 \pm j\}$  with equal probability (1/4) for each alphabet and the data length  $N = 2500$ . The initial condition  $\nu_0$  with  $v_{1,1}[n] = \delta[n - 12]$  and  $v_{1,2}[n] = 0$  was used by the SEA.

The simulation results corresponding to those shown in Figures 4(a), 4(b) and 4(c) are shown in Figures 5(a), 5(b) and 5(c), respectively. As drawn in Example 1, the SEA, the proposed LSEA-B and 2S-LSEA have similar performance, while the proposed 2S-LSEA converges (spending 2 iterations) faster than the other two algorithms (spending 3 iterations). These simulation results support the efficacy of the proposed LSEA-B and 2S-LSEA.

### V. Conclusions

We have presented three algorithms, LSEA-B, LSEA-F and 2S-LSEA for blind deconvolution of MIMO channels that share the merits of lattice structure as mentioned in (R1). The performance of the LSEA-B and 2S-LSEA in terms of ISI is similar to that of Yeung and Yau's SEA (see (R4)), and the convergence speed of the LSEA-B is also similar to that of Yeung and Yau's SEA while the 2S-LSEA converges fastest (see (R6)). The applications of the proposed three algorithms to wireless communications are currently under study.

### VI. References

- [1] O. Shalvi and E. Weinstein, *Universal Methods for Blind Deconvolution*, A chapter in *Blind Deconvolution*, S. Haykin, ed., Prentice-Hall, New Jersey, 1994.
- [2] O. Shalvi and E. Weinstein, "Super-exponential methods for blind deconvolution," *IEEE Trans. Information Theory*, vol. 39, no. 2, pp. 504-519, March 1993.

- [3] J. Gomes and V. Barroso, "A super-exponential algorithm for blind fractionally spaced equalization," *IEEE Signal Processing Letters*, vol. 3, pp. 283-285, Oct. 1996.
- [4] K.L. Yeung and S.F. Yau, "A cumulant-based super-exponential algorithm for blind deconvolution of multi-input multi-output systems," *Signal Processing*, vol. 67, pp. 141-162, 1998.
- [5] C.-C. Feng and C.-Y. Chi, "A two-step lattice super-exponential algorithm for blind equalization," Proc. 4th Symposium on Computer and Communications, Taoyuan, Taiwan, Oct. 7-8, 1998, pp. 329-335.
- [6] M.H. Hayes, *Statistical Digital Signal Processing and Modeling*, John Wiley and Sons, New York, 1996.
- [7] J.K. Tugnait, "Identification and deconvolution of multichannel linear non-Gaussian processes using higher order statistics and inverse filter criteria," *IEEE Trans. Signal Processing*, vol. 45, pp. 658-672, Mar. 1996.
- [8] B. Friedlander, "Lattice filter for adaptive filtering," *Proc. IEEE*, vol. 70, pp. 829-868, Aug. 1982.

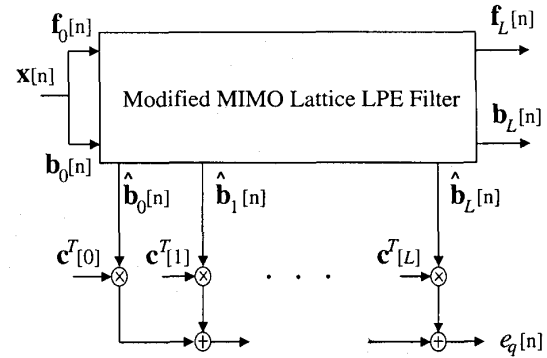


Figure 2. The proposed LSEA-B for MIMO channels.

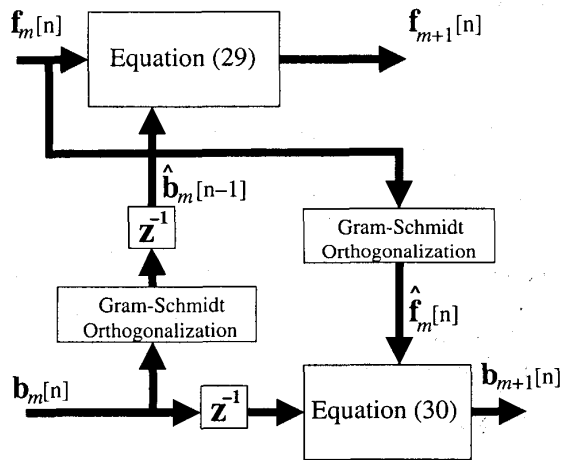


Figure 1. Stage  $m$  of the modified MIMO Lattice LPE filter.

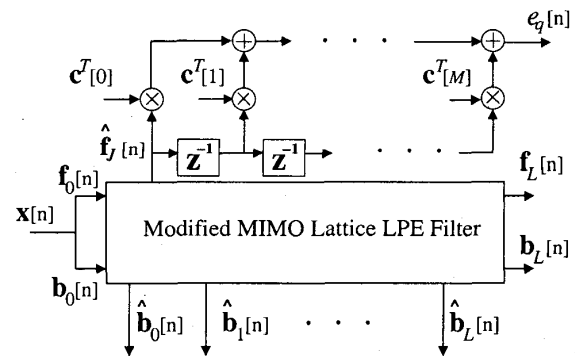


Figure 3. The proposed LSEA-F for MIMO channels.

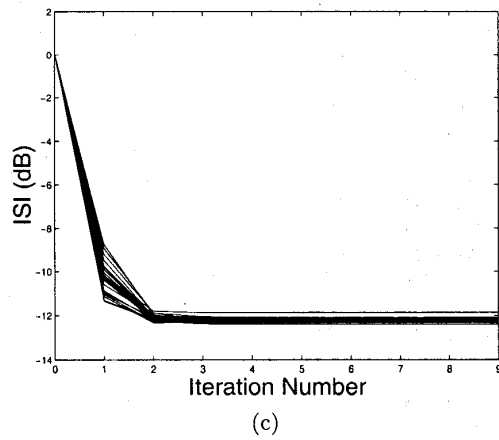
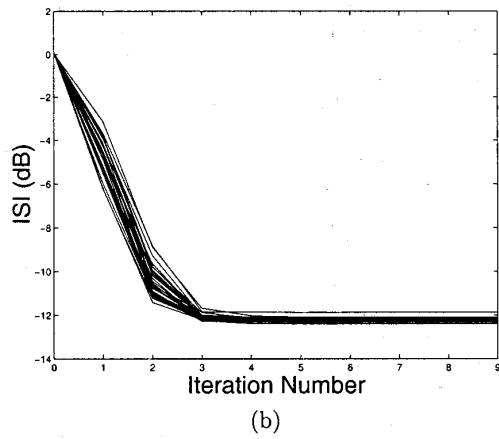
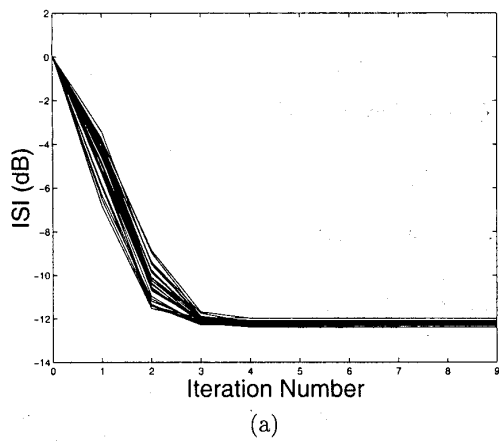


Figure 4. Simulation results of Example 1. ISI associated with (a) SEA, (b) LSEA-B and (c) 2S-LSEA.

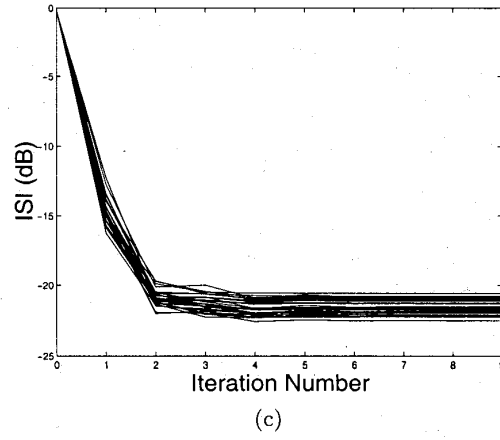
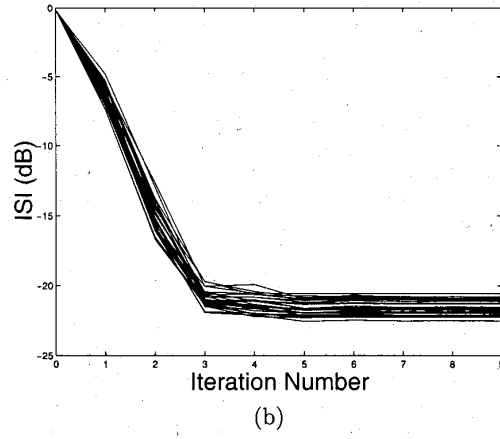
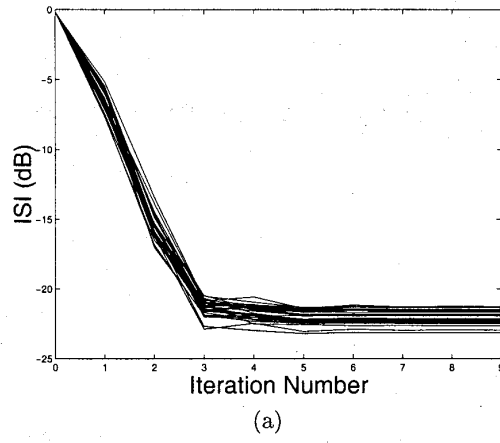


Figure 5. Simulation results of Example 2. ISI associated with (a) SEA, (b) LSEA-B and (c) 2S-LSEA.